© 2017. Published by The Company of Biologists Ltd | Journal of Experimental Biology (2017) 220, 2748-2756 doi:10.1242/jeb.154294

RESEARCH ARTICLE

Lowering metabolic rate mitigates muscle atrophy in western fence lizards

Jordan Balaban* and Emanuel Azizi

ABSTRACT

Extended periods of skeletal muscle disuse can cause a significant loss of contractile proteins, which compromises the ability to generate force, mechanical work or power, thus compromising locomotor performance. Several hibernating organisms can resist muscle atrophy despite months of inactivity. This resistance has been attributed to a reduction in body temperature and metabolic rate and activation of physiological pathways that counteract pathways of protein degradation. However, in these systems, such strategies are not mutually exclusive and the effects of these mechanisms can be difficult to separate. In this study, we used the western fence lizard, *Sceloporus occidentalis*, as an ectothermic model to determine whether a reduction in metabolic rate is sufficient to resist muscle atrophy. We induced atrophy through sciatic denervation of the gastrocnemius muscle and housed lizards at either 15 or 30°C for 6–7 weeks. Following treatment, we used muscle ergometry to measure maximum isometric force, the force–velocity relationship and contractile dynamics in the gastrocnemius. This approach allowed us to relate changes in the size and morphology to functional metrics of contractile performance. A subset of samples was used to histologically determine muscle fiber types. At 30°C, denervated muscles had a larger reduction in muscle mass, physiological cross-sectional area and maximum isometric force than at 15°C. Maximum shortening velocity of the muscle decreased slightly in animals housed at 30°C but did not change in those housed at 15°C. Our results suggest that metabolic rate alone can influence the rate of muscle atrophy and that ectothermic vertebrates may have an intrinsic mechanism to resist muscle atrophy during seasonal periods of inactivity.

KEY WORDS: *Sceloporus occidentalis*, Ectotherm, Skeletal muscle, Hibernation, Temperature

INTRODUCTION

The contractile and mechanical properties of skeletal muscles are plastic and readily change in response to changes in loading conditions. Extended bed rest, spinal or nerve injury, and extended periods of microgravity often result in a substantial loss of contractile protein (atrophy) in the skeletal muscles of humans. This loss of muscle mass can decrease the ability of muscles to generate force, mechanical work and mechanical power and in turn compromises locomotor performance, thereby increasing the risk of predation and decreasing prey capture success.

Department of Ecology and Evolutionary Biology, University of California, Irvine, Irvine, CA 92697, USA.

*Author for correspondence (jbalaban@uci.edu)

J.B., 0000-0003-2848-5444

Received 5 December 2016; Accepted 10 May 2017

Atrophy does not impact all muscles, or even muscle fibers, equally. In atrophied muscles, slow oxidative fibers have a decreased cross-sectional area (CSA) (Caiozzo et al., 1994; Ohira et al., 2002), and represent a smaller proportion of the overall fibers compared with healthy muscle (Caiozzo et al., 1996). In contrast, larger, fast glycolytic fibers and intermediate fast glycolytic/oxidative fibers tend to maintain their CSA and either maintain or increase as a proportion of fibers within a muscle (Caiozzo et al., 1994, 1996; Ohira et al., 2002). This pattern of remodeling results in an increase in maximal contractile speed along with a decrease in force (Caiozzo, 2002). The rates and patterns of atrophy can vary based on the frequency and pattern of recruitment prior to a disuse signal. This is thought to explain why slow oxidative fibers, which are recruited more frequently even at submaximal levels of activation, are more prone to atrophy. This pattern can be extended to comparisons of different muscles, where muscles with similar fiber-type distributions atrophy at different rates if one was activated more frequently prior to disuse (Lieber, 2002). Therefore, a muscle's propensity to atrophy in response to a disuse stimulus depends on a number of factors: the relative decrease in use, fiber-type composition, metabolic rate and the method used to induce atrophy (Caiozzo, 2002; Lieber, 2002; Winiarski et al., 1987; Hudson and Franklin, 2002).

Some animals have evolved mechanisms to slow the rate of muscle disuse atrophy despite months of inactivity. Hibernating animals often remain completely inactive through the winter but suffer little or no loss in muscle performance. Many hibernating mammals are able to maintain a large percentage of their pre-hibernation muscle mass (James et al., 2013; Lin et al., 2012; Rourke, 2004; Wickler et al., 1991) and force (James et al., 2013; Lohuis et al., 2007). In hibernating ground squirrels, the ratios of different fiber types do not follow the typical pattern of mammalian atrophy and remain largely unchanged or are shifted towards a larger proportion of slow oxidative fibers (Rourke, 2004; Xu et al., 2013). Given the impressive ability of hibernating organisms to resist atrophy, there has been an increasing focus on investigating the underlying mechanisms used to retain muscle mass and performance during long periods of disuse. Some hibernating mammals can lower their body temperature and suppress their metabolic rate below what would be expected given the Q_{10} of metabolic reactions (Geiser, 2004; Muleme et al., 2006; Staples, 2014). Additionally, hibernating ground squirrels have been shown to activate the PGC-1α-mediated exercise pathway to prevent muscle atrophy and shift muscle fibers towards fatigue resistance (Xu et al., 2013). Antioxidant production has also been shown to be up-regulated in hamsters during brief periods of arousal from hibernation (Ohta et al., 2006; Okamoto et al., 2006), as well as in Australian burrowing frogs aestivating at high temperatures (Young et al., 2013). The up-regulation of antioxidants can counteract the reactive oxygen species that increase the rate of proteolysis through mechanisms such as the ubiquitin–proteasome system (Powers

Journal of Experimental Biology

Journal of Experimental Biology (2017) 220, 2748-2756 doi:10.1242/jeb.154294

List of symbols and abbreviations

CSA	cross-sectional area
FG	fast glycolytic
FOG	fast oxidative/glycolytic
L_0	muscle length at maximal twitch force
L_f	fiber length
M_b	body mass
M_{muscle}	muscle mass
P_0	maximum isometric force
PCSA	physiological cross-sectional area
SMR	standard metabolic rate
SO	slow oxidative
SVL	snout–vent length
V_{max}	maximum shortening velocity
θ	pennation angle
ρ	muscle density

et al., 2007; Bonaldo and Sandri, 2013; Schiaffino et al., 2013). These diverse strategies of metabolic rate suppression, antioxidant production and exercise pathway activation appear to provide hibernating organisms with the unique ability to mitigate muscle atrophy despite significant periods of inactivity.

The various strategies used by animals to resist muscle atrophy during hibernation are not mutually exclusive and a given animal may combine a number of strategies to maintain muscle function. Consequently, it is difficult to analyze the individual contribution of any one of these strategies. We aimed to functionally decouple the effect of metabolic rate from the effect of other physiological pathways activated during mammalian hibernation to determine whether a reduction in metabolic rate alone is sufficient to mitigate muscle atrophy. We used the western fence lizard, *Sceloporus occidentalis*, as an ectothermic model organism to control metabolic rate via ambient temperature, while applying a disuse stimulus by denervating the gastrocnemius muscle. As mammalian muscle from non-hibernators follows a distinct pattern of atrophy, we also used this system to investigate whether the muscles of lizards follow the same pattern of atrophy as mammalian muscle. To address these questions, we quantified and compared the size, morphology, contractile properties and fiber-type composition in the gastrocnemius muscle of control animals and denervated animals housed at 15 and 30°C. Hibernating animals can suppress their metabolic rate to a lower level than temperature alone would predict (Staples, 2014). This yields a Q_{10} much greater than 2, which is the approximate Q_{10} of metabolic rate in animals. Thus, if the lizards housed at 15°C enter a hibernation-like state over the course of this study, then we would expect the Q_{10} between 15 and 30°C to be higher than 2.3, which is the unacclimated Q_{10} of *S. occidentalis* between 20 and 30°C (Dawson and Bartholomew, 1956). If the Q_{10} remains low, this would suggest our temperature perturbation only affects metabolic rate. Our intention was to relate metabolic rate to the rate at which skeletal muscle remodels and broaden our understanding of skeletal muscle plasticity in ectothermic organisms. If lizard muscle atrophies similarly to mammalian muscle, we predict that denervated muscles from animals housed at 30°C would show a reduction in muscle mass, muscle physiological cross-sectional area (PCSA), maximal contractile force, muscle fiber CSA and proportion of fast glycolytic fibers when compared with control muscles. We also predict a higher maximal contractile velocity in denervated muscles from lizards housed at 30°C compared with control muscles. If a reduced metabolic rate mitigates muscle atrophy, we hypothesize little to no difference between denervated and control muscles from lizards housed at 15°C.

MATERIALS AND METHODS

Animals

Thirty-six western fence lizards, *Sceloporus occidentalis* Baird and Girard 1852 (10.13±3.15 g, mean±s.d.), were caught on the University of California, Irvine, campus using a California Department of Fish and Wildlife scientific collectors permit SC-12906 (issued to J.B.). Lizards were housed individually in terraria with a sandy substrate, given water *ad libitum* and fed crickets supplemented with calcium. Before treatment began, lizards were given a UV light and a heating lamp on a 12 h:12 h light:dark cycle to provide a thermal gradient to allow for thermoregulation. In the treatments, lizards were housed at either 15 or 30°C with a UV light on a 12 h:12 h light:dark cycle, but no heating lamp to ensure constant metabolic rates. This work was carried out at UC Irvine under Institutional Animal Care and Use Committee protocol no. 2013-3110.

Denervation

We used the medial gastrocnemius, a major ankle extensor, for all experimental protocols. To denervate the muscle, lizards were anesthetized with 5% isoflurane for at least 10 min, and until the self-righting and toe-pinch reflexes were no longer present. A small dorsal incision was made on the posterior portion of hindlimb (where the thigh meets the trunk). Ceramic-coated forceps were then inserted in between the iliofibularis and ilioischiotibialis muscles to grasp the sciatic nerve, which was isolated and pulled free from the surrounding structures (Fig. 1A). A section of the sciatic nerve no less than 2 mm in length was then removed to prevent regrowth of the nerve within the 6 week experimental period. Sham surgeries were performed on control limbs following the same procedure as the denervated group but without extracting and cutting the sciatic nerve. Sutures (6-0 silk) were used to close the incision. These surgical procedures were performed under semi-sterile conditions. Lizards were allowed to recover for 2 days in a cage with a 12 h:12 h light:dark cycle with UV broad-spectrum light (Exo Terra Repti Glo 2.0) and a heating bulb (Exo Terra Sun Glo Basking Spot Lamp, 75 W) placed above one side of the cage to allow for behavioral thermoregulation. After recovery, lizards were placed in new cages with a sandy substrate and the cages were placed randomly into either a 15°C (N=18) or 30°C (N=18) environmental chamber for 6 weeks. A period of 6 weeks was chosen as it was long enough to elicit significant muscle atrophy, but not so long as to negatively impact animal health.

Metabolic rate

To ensure that cold-housed lizards were not hibernating, we measured the metabolic rate during the fifth week of acclimation using a subsample of lizards from the 15 and 30°C groups (N=3 and N=5, respectively). We placed the lizards into a 108 ml chamber housed in a temperature-controlled cabinet at 17°C for the cold-incubated lizards or 30°C for the warm-incubated lizards. Metabolic rates were measured at 17°C instead of 15°C, as that was the lowest temperature our metabolic chamber could reach. Q_{10} measurements should not be affected by this slight difference in temperature, and less than 24 h at this slightly elevated temperature should not have an effect on rates of muscle atrophy over 6 weeks. Room air scrubbed of CO_2 and H_2O was passed through a long coiled copper tube inside the temperature cabinet to bring the air to the correct temperature. After the coil, the air was passed through the chamber

Journal of Experimental Biology (2017) 220, 2748-2756 doi:10.1242/jeb.154294

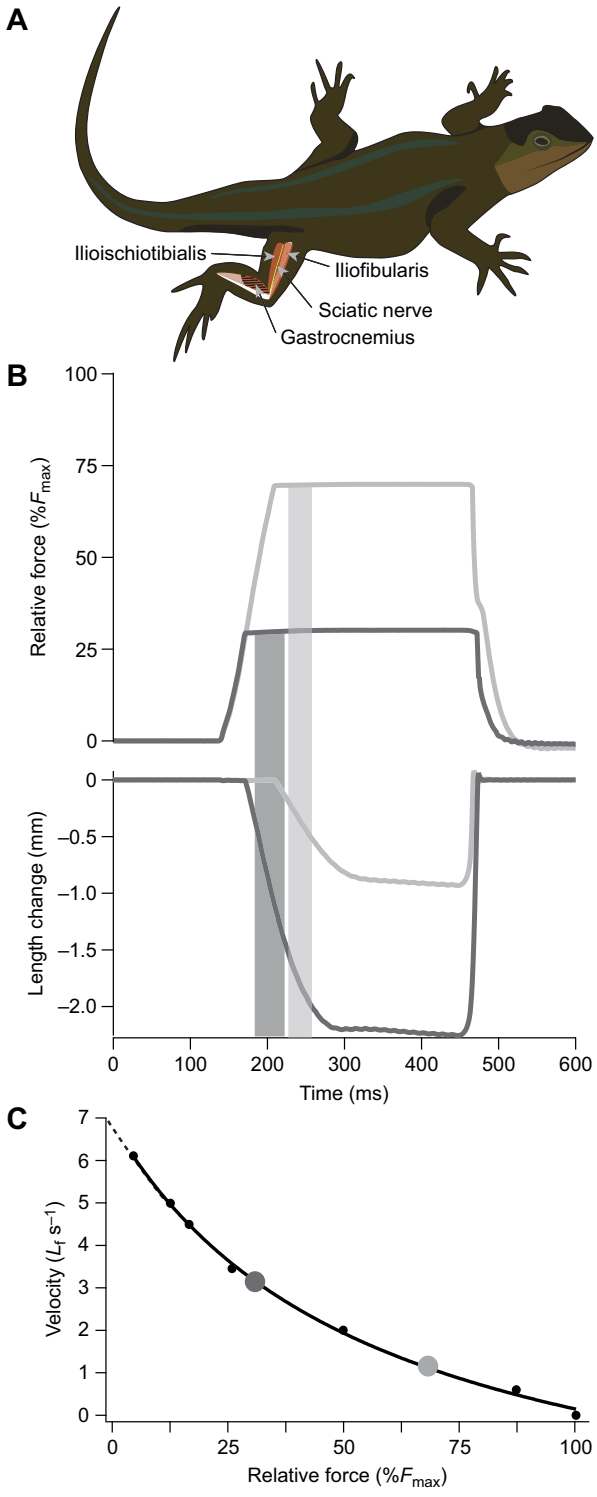

Fig. 1. Experimental design. (A) Leg anatomy of the western fence lizard. An incision was made on the dorsal proximal thigh and the sciatic nerve was severed to denervate the medial gastrocnemius muscle. (B) Representative time series traces showing force (relative to maximum force, F_{max}) and length during two isotonic contractions at 30% and 70% of maximum contractile force (P_0). Gray vertical bars indicate the time at which force and velocity measurements were taken for each contraction. (C) Force–velocity relationship for a representative muscle characterized using a series of isotonic contractions between 5% and 100% of P_0. The contractions shown in B are indicated with large circles. The force–velocity data were fitted with a hyperbolic–linear equation (Marsh and Bennett, 1986). L_f, fiber length.

housing the lizard at a rate of 100 ml min^{-1}. Once it had passed over the lizards it was again scrubbed of H_2O and passed through a CO_2 gas analyzer (model 6262, Li-Cor Inc., Lincoln, NE, USA). Data were collected using ExpeData software (Sable Systems) for at least 12 h, until the metabolic rate remained constant for at least 1 h. Data from the constant portion of the curve were used to calculate the standard metabolic rate (SMR, in ml CO_2 g^{-1} h^{-1}). The Q_{10} of the lizards was calculated as the change in SMR over 10°C using the equation:

$$Q_{10} = \left(\frac{\mathrm{SMR}_{30}}{\mathrm{SMR}_{17}}\right)^{10/\Delta T}. \quad (1)$$

In vitro muscle preparation

Lizards were killed via an overdose of 5% inhaled isoflurane followed by a double-pithing protocol. Medial gastrocnemius muscles were isolated and the distal tendon was separated from the ankle. The femur immediately proximal to the knee and the tibia and fibula immediately distal to the knee were cut, along with all of the muscles aside from the medial gastrocnemius. Kevlar thread was then tied around the origin of the muscle, immediately distal to the knee. The other end of the thread was attached to a dual-mode servomotor (Aurora Scientific 360C, Cambridge, MA, USA). The distal tendon of the muscle was fixed in place via a small screw clamp mounted to an aluminium post. Sandpaper (150 grit) was affixed to the inside edges of the clamp to prevent the tendon from slipping. Muscles were bathed in a 23°C oxygenated Ringer's solution (100 mmol l^{-1} NaCl, 2.5 mmol l^{-1} KCl, 2.5 mmol l^{-1} $NaHCO_3$, 1.6 mmol l^{-1} CaCl, 10.5 mmol l^{-1} dextrose) for the duration of the experiment.

Contractile data were collected using a 16-bit data acquisition system (National Instruments, Austin, TX, USA). Data were collected at 1000 Hz and analyzed using Igor Pro software (v 6.22A, Wavemetrics, Lake Oswego, OR, USA). A series of twitch contractions was used to determine optimal voltage (between 50 and 70 V using parallel platinum plate electrodes) to supramaximally stimulate the muscle. Another series of twitch contractions was used to determine the force–length relationship of the muscle. Tetanic contractions were achieved using a stimulation pulse duration of 0.2 ms and a frequency of 80 pulses s^{-1} for 400 ms. A tetanic contraction starting at the optimal length of the twitch force–length curve (L_0) was used to determine maximum isometric force (P_0). A series of isotonic tetanic contractions was used to characterize the force–velocity relationship of each muscle (Fig. 1B). After force developed to a preset value, it was maintained by the servomotor and the muscles shortened. Force–velocity curves were characterized for each muscle from 7–10 isotonic contractions ranging from 5% to 90% of P_0. We elicited an isometric contraction in the middle and at the end of each experiment to ensure no drop in P_0. Any muscle where maximum isometric force fell below 85% of the initial P_0 was removed from the analysis. Once all contractions were completed, muscle length at L_0 and wet mass were measured. Muscles were then fixed at L_0 in 10% formalin for fiber length and pennation angle measurements.

We obtained velocity measurements from each contraction by calculating the average change in muscle length divided by the duration of the constant velocity portion of muscle shortening. Force measurements were taken as the average force for the period of time over which velocity measurements were taken (Fig. 1B). To characterize the force–velocity properties of the gastrocnemius, we plotted force and the corresponding shortening velocity and fitted

Journal of Experimental Biology

Journal of Experimental Biology (2017) 220, 2748-2756 doi:10.1242/jeb.154294

the following hyperbolic–linear equation to the data as an alternative to the Hill equation (Marsh and Bennett, 1986):

$$V = \frac{B(1-F)}{(A+F)} + C(1-F),$$

where V is velocity (in fascicle lengths per second), F is force (in N), and A, B and C are constants that are iteratively adjusted to fit the force–velocity data (Fig. 1C).

Morphology

To characterize the degree of muscle atrophy, we measured muscle mass and PCSA. Following *in vitro* characterization of contractile properties, gastrocnemius muscles were submerged in 10% formalin solution for 10 min to partially fix them at their optimal length for force production (L_0). Muscles were then patted dry using a paper towel until there were no apparent wet marks on the paper. We weighed the muscles to the nearest 0.001 g and then stored them in formalin to continue the fixation process. Fiber length (L_f) was obtained by dissecting out fibers from fixed tissue and measuring them using a set of electronic calipers. Average values of three fibers taken from different areas of the muscle were used as average L_f. We took images of the muscles using a digital camera attached to a dissecting microscope (AMscope, mu500, Irvine, CA, USA). Pennation angle (θ) was then taken from these images using ImageJ software (NIH, Bethesda, MD, USA). We took the angle as the average of the angles between the central tendon and the fibers to its right and left.

We calculated PCSA using the equation:

$$\text{PCSA} = \frac{M_{\text{muscle}} \times \cos\theta}{\rho \times L_f},$$

where M_{muscle} is muscle mass, ρ is muscle density (1.06 g cm^{-2}), a value taken from the literature (Biewener, 2002), and θ is the pennation angle of the muscle measured relative to the line of action.

Histology

We flash froze gastrocnemius muscles in isopentane cooled with liquid nitrogen. Muscles were pinned when the ankle and knee joints were in 90 deg flexion to ensure consistency of lengths before freezing. Muscle cross-sections were prepared with a cryotome at −24°C (12 µm). Sections were taken perpendicular to fiber orientation for accurate comparison of fiber cross-sections. These sections were allowed to dry for 12–24 h. We then stained for both NADH dehydrogenase and alkali-stable mATPase to visualize the oxidative and glycolytic capacities of the muscle using an established protocol for lizard muscle (Moritz and Schilling, 2013). A histology staining kit (Scientific EasyDip Slide staining system, Simport, Montreal, QC, Canada) was used to stain the sections.

Two cross-sections taken at different locations along the muscle were imaged per muscle using a high-powered dissecting microscope with a camera attached (Discovery V20, Zeiss). Individual fibers were identified as fast glycolytic (FG), fast oxidative/glycolytic (FOG) and slow oxidative (SO) by the presence of the diffuse brown stain for mATPase (FG), the dark blue stain of NADH dehydrogenase in the mitochondria (SO) or the two stains simultaneously (FOG) (Fig. 2). Individual fibers were counted within each section, and the total number of each fiber type was averaged across sections. The CSA of a representative subsection from each section of muscle was measured using ImageJ software (NIH). Fiber CSAs within this subsection were then measured to determine the average CSA of each fiber type. To indirectly measure the collagen content of the muscles, the proportion of the cross-section that was not composed of muscle fibers was measured as the total CSA of a subsection minus the sum of the CSAs of the fibers in that subsection divided by the total CSA of the subsection. Only clean sections without artifacts due to flash-freezing or cryosectioning were used for the CSA analyses.

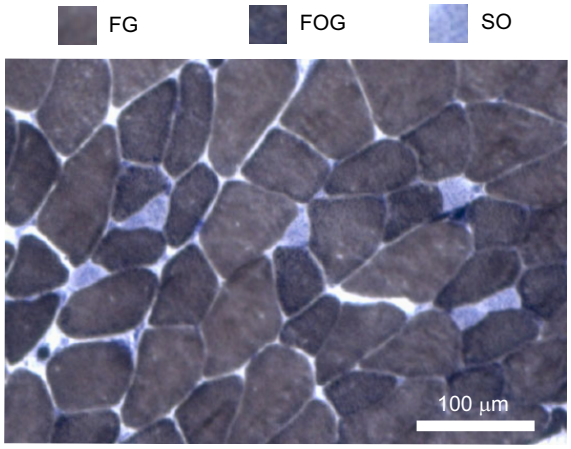

Fig. 2. Representative histology section from double-stained gastrocnemius muscles. Fast glycolytic (FG) fibers stained only for alkali-stable myosin ATPase. Slow oxidative (SO) fibers stained only for NADH dehydrogenase. The intermediate fast oxidative/glycolytic (FOG) fibers stained for both alkali-stable myosin ATPase and NADH dehydrogenase.

Statistics

All statistical analyses were performed in R (http://www.R-project.org/). Using the lme4 (Bates et al., 2015) and car (Fox and Weisberg, 2011) packages, we ran linear mixed effects (LME) models on all morphological, contractile and histological variables to test for differences between denervated and control muscles at 15 and 30°C. Individual was used as a random variable in all tests to account for individual variation and because some lizards were unilaterally denervated with the contralateral limb as a sham surgery control, and others were bilaterally denervated or bilaterally given a sham surgery. In the analyses of M_{muscle} and P_0, we included body mass (M_b) as a covariate; in the PCSA analysis, we included the square of snout–vent length (SVL^2) as a covariate; and in our analysis of maximum shortening velocity (V_{max}), L_f was included as a covariate. We compared metabolic rate data between temperature groups using Student's *t*-test.

RESULTS

Metabolic rate

The average $\dot{V}_{CO_2}$ was 0.56±0.05 ml CO_2 kg^{-1} min^{-1} (mean±s.e.m., N=3) for lizards housed at 15°C for 6 weeks (tested at 17°C), and 1.47±0.12 ml CO_2 kg^{-1} min^{-1} (N=5) for lizards housed at 30°C for 6 weeks. Metabolic rate differed significantly between the two temperature groups (P=0.001, Student's *t*-test), with a Q_{10} of 2.08 for metabolic rate across this temperature range. This result is similar to findings of a previous study, which measured a slightly higher Q_{10} of 2.3 for *S. occidentalis* between 20 and 30°C (Dawson and Bartholomew, 1956), and confirms that experimental animals held at 15°C were not suppressing their metabolic rate, unlike hibernating mammals. If they were, we would expect Q_{10} values to be higher than the previously recorded value of 2.3. This indicates that fence lizards may not be activating other atrophy-prevention

Journal of Experimental Biology (2017) 220, 2748-2756 doi:10.1242/jeb.154294

Table 1. Morphological and contractile data

	15°C		30°C	
	Control	Denervated	Control	Denervated
M_{muscle} (mg)	35.95±4.28 (14)	32.83±4.53 (9)	34.53±2.89 (14)	31.22±3.02 (13)
M_b (g)	10.46±1.06 (14)	10.13±1.15 (10)	11.44±0.81 (13)	11.85±1.05 (13)
P_0 (N)	1.14±0.11 (12)	0.93±0.12 (6)	1.05±0.08 (8)	0.93±0.10 (5)
Power (W)	$4.8\times10^{-3}\pm5.84\times10^{-4}$ (12)	$3.53\times10^{-3}\pm5.46\times10^{-4}$ (6)	$4.40\times10^{-3}\pm3.59\times10^{-4}$ (8)	$3.57\times10^{-3}\pm3.29\times10^{-4}$ (5)
PCSA (mm^2)	7.07±0.77 (12)	6.59±0.91 (8)	7.02±0.58 (9)	6.50±0.60 (9)
SVL (mm)	66.69±1.84 (14)	66.49±2.07 (10)	69.66±1.31 (14)	70.05±1.80 (14)
V_{max} (mm s^{-1})	28.48±1.06 (10)	28.99±1.91 (4)	30.51±1.15 (8)	28.88±1.29 (6)
L_f (mm)	4.69±0.13 (13)	4.61±0.14 (9)	4.61±0.15 (10)	4.70±0.12 (10)

Data (means±s.e.m. with sample size in parentheses) are for all morphological and contractile measurements. M_{muscle}; M_b, body mass; P_0, maximum contractile force; PCSA, physiological cross-sectional area; SVL, snout–vent length; V_{max}, maximum shortening velocity; L_f, fiber length.

pathways and that any effects on atrophy are solely a result of changes in metabolic rate.

Morphology

Gastrocnemius M_{muscle} was lower in denervated lizards (N=13) than in controls (N=14) at 30°C (P<0.001, LME model with M_b as a covariate and individual as a random effect; Table 1). In lizards housed at 15°C, denervated gastrocnemius M_{muscle} (N=9) was smaller than that of controls (N=14, P=0.031, LME model with M_b as a covariate and individual as a random effect; Table 1). When corrected for M_b, denervated M_{muscle} was 14% smaller than that of controls in lizards housed at 30°C and 3% smaller in lizards housed at 15°C (Fig. 3A). There was a trend showing a possible interaction effect between temperature and denervation for M_{muscle} (P=0.058).

PCSA was lower in denervated lizards (N=9) than in controls (N=9) at 30°C (P=0.001, LME model with SVL^2 as a covariate and individual as a random effect; Table 1). PCSA of denervated (N=8) gastrocnemius muscles in lizards housed at 15°C was lower than that of controls (N=12, P=0.048, LME model with SVL^2 as a covariate and individual as a random effect; Table 1). When corrected for SVL^2, denervated muscles had 11% smaller PCSA than controls in lizards housed at 30°C and 6% smaller PCSA in lizards housed at 15°C (Fig. 3B).There was an interaction effect between temperature and denervation for PCSA (P=0.025).

Contractile properties

Gastrocnemius denervation resulted in lower P_0 at 30°C (P=0.004, LME model with M_b as a covariate and individual as a random effect, N=5 and 8, respectively, for denervated and control; Table 1) and at 15°C (P=0.045, LME model with M_b as a covariate and individual as a random effect, N=6 and 12, respectively, for denervated and control; Table 1). When corrected for M_b, denervated muscles produced 17% lower force than controls in lizards housed at 30°C and 8% lower force in lizards housed at 15°C (Figs 3C and 4). There was no interaction between temperature and denervation for P_0 (P=0.596).

V_{max} was slower in denervated lizard muscles than in controls at 30°C (N=6,8, P=0.040, LME model with L_f as a covariate and individual as a random effect; Table 1). When corrected for L_f, this difference was 6% (Figs 3D and 4A). No difference was detected in the V_{max} of gastrocnemius muscles in lizards housed at 15°C (P=0.853, LME model with L_f as a covariate and individual as a random effect; Table 1). There was no interaction effect between temperature and denervation for V_{max} (P=0.442).

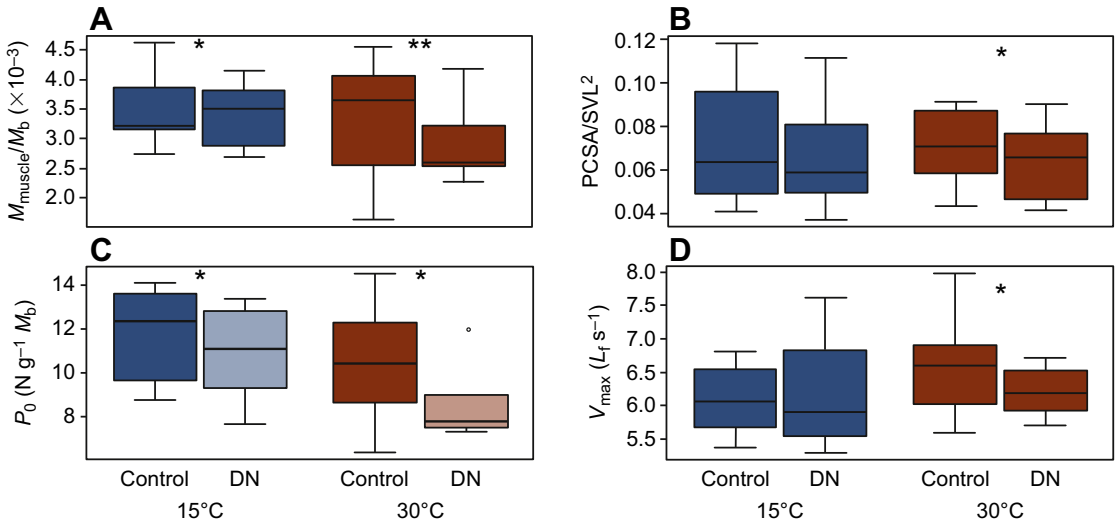

Fig. 3. Morphological and contractile data from all treatments. Box plots represent the median, minimum, 25th percentile, 75th percentile and maximum data points (circle indicates an outlier). Muscle mass/body mass (M_{muscle}/M_b; A), physiological cross-sectional area/snout–vent length^2 (PCSA/SVL^2; B) and maximal isometric force (P_0; C) corrected for body mass were all around 15% lower and maximum shortening velocity (V_{max}; D) was 6% lower in denervated muscles (DN) from lizards housed at 30°C (N=13, 9, 5 and 6, respectively). P_0 (N=5; C) was 8% lower and M_{muscle}/M_b (N=9; A) was 3% lower in denervated muscles from the 15°C group, but PCSA/SVL^2 (N=8; B) and V_{max} (N=7; D) were similar to controls. *P<0.05, **P<0.001.

Journal of Experimental Biology

Journal of Experimental Biology (2017) 220, 2748-2756 doi:10.1242/jeb.154294

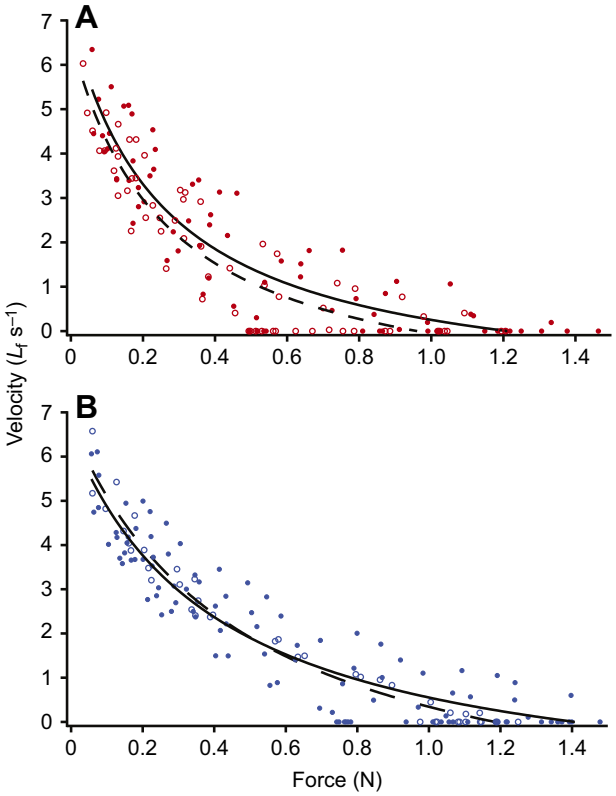

Fig. 4. Summary of force–velocity data from all lizards housed for 6 weeks at 30 and 15°C. Open symbols indicate denervated muscles and filled symbols indicate control muscles. Average force–velocity fits for data from denervated muscles (dashed lines) and control muscles (solid lines) are shown. Velocities are presented corrected for L_f and force is presented as absolute values (N). (A) P_0 corrected for M_b was 13% lower in denervated muscles (N=6). V_{max} was 6% slower in denervated muscles. (B) Corrected P_0 was 10% lower in denervated muscles (N=7), but we found no difference in V_{max}.

Histology

The CSA of FG (control 4121±1332 μm^2, N=8; denervated 3482±1138 μm^2, N=7, P=0.34) and FOG (control 2770±916 μm^2, N=8; denervated 2519±914 μm^2, N=7, P=0.60) fibers was not different in control and denervated muscles (Fig. 5A) in the 30°C group. However, individual SO fibers were, on average, 36% larger in the denervated gastrocnemius muscles (655.58±76.09 μm^2, N=7) of lizards housed at 30°C than in controls (483.10±27.54 μm^2, N=8; P=0.04; Fig. 5A). We did not detect any differences between denervated and control muscles in the percentage of CSA not composed of muscle fibers. There was a trend toward a 10% larger proportion of FG fibers in denervated muscles (74.71±3.29%, N=7) than in control muscles at 30°C (67.85±2.18%, N=8, P=0.098; Fig. 5B). The proportion of FOG fibers was lower in denervated (18.03±2.68%) muscles than in control muscles at 30°C (25.74±2.38%, P=0.05; Fig. 5B). The proportion of SO fibers was not different between groups at 30°C (P=0.46, Fig. 5B).

FG (P=0.88), FOG (P=0.87) and SO (P=0.14) fibers were not significantly different in CSA between denervated (N=5) and control (N=4) muscles of lizards housed at 15°C. Likewise, there was no difference between denervated and control muscles in the proportion of CSA not composed of muscle fibers. Additionally, we found no differences in the proportion of FG (P=0.75), FOG (P=0.79) and SO (P=0.68) between denervated and control muscles at 15°C (Fig. 5B).

DISCUSSION

Lizards housed at 15°C had a lower metabolic rate than lizards housed at 30°C corresponding to a Q_{10} of 2.08, which is in line with that found previously in western fence lizards (Dawson and Bartholomew, 1956). Though some hibernating animals have additional mechanisms to avoid atrophy, all hibernating and aestivating animals activate mechanisms that suppress metabolic rate (Tessier and Storey, 2016; Hudson and Franklin, 2002). Our measured Q_{10} of 2.08 suggests that no animals housed at 15°C were activating any additional hibernation pathways to limit atrophy. After 6 weeks, denervated gastrocnemius muscles from 30°C lizards showed substantial decreases in mass, force, PCSA and V_{max} compared with control muscles (Figs 3 and 4). In 15°C lizards, we found no differences between groups in muscle CSA or V_{max}, while muscle mass and force were reduced in the denervated muscles, though not as severely as for the 30°C groups. We propose that the different responses to denervation seen in the two groups are due to differential rates of muscle protein degradation in direct response to the lower metabolic rate of the cool lizards.

Much of what we know about muscle atrophy is based on studies of mammals. The typical pattern of muscle atrophy in mammals is described by a loss of contractile proteins, which unsurprisingly results in a lower P_0. Less intuitively, V_{max} of atrophied muscles increases, as does muscle fatigability. This shift is partly because slow oxidative fibers are recruited at all levels of activation and therefore face a substantial reduction in their level of activity in response to a disuse stimulus. In addition, fatigue-resistant slow oxidative fibers have an abundance of mitochondria, are highly metabolically active, and produce relatively large levels of reactive oxygen species as a byproduct of oxidative phosphorylation. This likely causes relatively rapid atrophy of fatigue-resistant slow muscle fibers in comparison to the fast fibers and, in some cases, transitions from slow to fast fibers. This remodeling leads to an increase in muscle speed and fatigability with atrophy (Caiozzo, 2002; Lieber, 2002). While these findings generally hold true, they are largely based on a few species of endothermic mammals with high and steady metabolic rates, namely rats, cats and humans (Caiozzo, 2002; McDonagh et al., 2004). In addition, many of the seminal studies using space flight, hindlimb suspension or limb immobilization to induce atrophy document the most significant and impressive changes in the soleus muscle, which is predominantly composed of slow twitch fibers (Booth, 1982; Caiozzo, 2002). While these studies have provided important insight into the conditions that induce atrophy and the functional consequences of disuse, it is difficult to extend the generality of the findings to other muscles or other species. When comparing a wide variety of vertebrates, the process of skeletal muscle atrophy and an organism's response to a disuse stimulus can be highly variable. Patterns of atrophy can vary based on muscle fiber type and the pattern of muscle use (Caiozzo, 2002; Lieber, 2002; Winiarski et al., 1987), metabolic rate (Hudson and Franklin, 2002), gene expression (Bodine, 2013; Xu et al., 2013), the method of inducing muscle atrophy (Fitts et al., 1986; Lieber, 2002; McDonagh et al., 2004), and even the metric used to quantify atrophy (Mantle et al., 2009). Even when comparing individual muscles within a single animal, the patterns and severity of atrophy can vary significantly. For example, in aestivating frogs, the response of four hindlimb muscles varies significantly after more than 6 months of disuse (Mantle et al., 2009). The observed differences between muscles are made more complicated by the fact that commonly used indicators of atrophy such as fiber CSA, muscle CSA, M_{muscle}, maximal force production, maximal power production and total protein content do

Journal of Experimental Biology (2017) 220, 2748-2756 doi:10.1242/jeb.154294

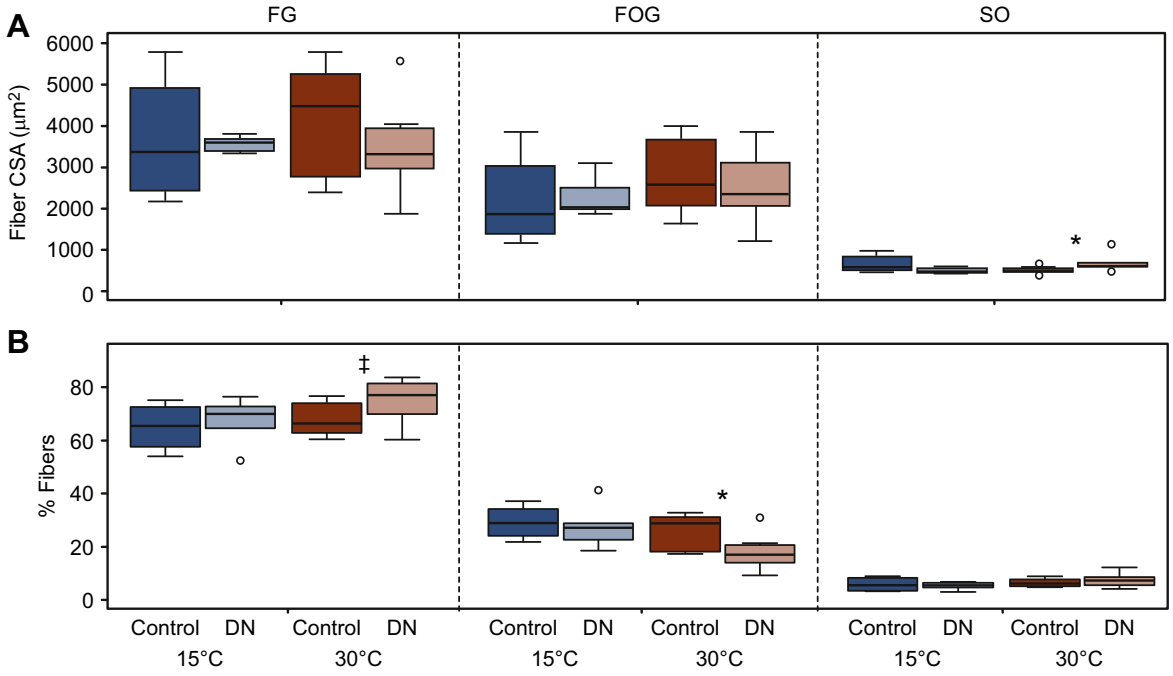

Fig. 5. Histological data from all treatments. Box plots represent the median, minimum, 25th percentile, 75th percentile and maximum data points (circles indicate outliers). (A) Box plots of fiber cross-sectional area (CSA) of FG, FOG and SO fibers. SO fibers were 36% larger in denervated muscles from lizards housed at 30°C (P=0.04). No other differences were significant at 15°C (N=4) or 30°C (N=7), but note that the average CSA of FG fibers was about 15% smaller in denervated muscles from the 30°C group. (B) Proportion of the total fiber population composed of FG, FOG and SO fibers. The proportion of FOG fibers was 30% smaller and there was a trend for a 10% larger proportion of FG fibers in denervated muscles from lizards housed at 30°C. *P=0.05, ‡P<0.10.

not change at the same rate and often indicate divergent outcomes. In the same study of atrophy in aestivating frogs, Mantle et al. (2009) noted that the iliofibularis muscles had significantly lower M_{muscle}, a smaller whole-muscle CSA and fiber CSA whereas the sartorius muscles had lower M_{muscle} and whole-muscle CSA with no changes in fiber CSA, the gastrocnemius muscles had only a decrease in whole-muscle CSA, and the cruralis muscles only had decreases in fiber diameter (Mantle et al., 2009).

The variation in the response of a muscle can also depend on the disuse protocol used in the study. For instance, denervation often leads to an initial period of hypertrophy of muscle fibers due to swelling of the tissue, despite a disorganization of contractile proteins which likely leads to an overall loss of force (Jirmanová and Zelená, 1970; Hikida and Bock, 1972). Though denervation does not always lead to muscle fiber hypertrophy (Bakou et al., 1996; Lin et al., 2012), it could explain the relatively larger drop in force compared with M_{muscle} observed in our 15°C denervated lizards (Fig. 3). In contrast to studies using denervation, experimental manipulations such as hindlimb suspension and microgravity often result in a decrease in force and muscle fiber diameter, though the time course of remodeling may again vary between the two methods (Winiarski et al., 1987; Fitts et al., 1986; Caiozzo et al., 1994). The observed level of variation in response to a disuse stimulus suggests that properties of the muscle, the time course of the response, the protocol used to induce atrophy and the metric used to characterize atrophy can all obscure the general relationship between the phenotypic response and the underlying mechanisms of atrophy.

In this study, we focused on understanding how the differences in metabolic rate can induce variation in the rate of muscle atrophy. We combined our results with data from previous studies in order to quantify the relationship between mass-specific metabolic rate and the rate of muscle atrophy (Fig. 6). This analysis is a modified and updated version of a previously performed analysis (Hudson and Franklin, 2002). To account for the variation between animals, muscles, perturbations and metrics, we only included the highest rates of atrophy measured in each study, which enabled us to minimize the inherent variation in the response of different muscles from different species using different experimental manipulations to induce atrophy. This analysis allowed us to compare hibernating and non-hibernating endotherms and ectotherms with various atrophy-inducing perturbations and metrics of atrophy. We found that, across vertebrates, there was a significant relationship between mass-specific metabolic rate and the rate of muscle atrophy, regardless of disuse condition, which muscle was used or whether the organism was an endotherm or ectotherm (R^2=0.95, P<0.05; Fig. 6). This pattern holds true despite the fact that our analysis includes a number of aestivating and hibernating species, which may be activating other atrophy-resistance pathways. Despite the significant variation observed in studies of muscle atrophy, our analysis indicates that metabolic rate is a strong predictor of muscle atrophy across vertebrates.

Though metabolic rate seems to drive the rate of muscle atrophy, other mechanisms used by hibernating and aestivating animals are likely to alter the patterns of atrophy. Many hibernators and aestivators can suppress their metabolic rate lower than a decrease in body temperature alone would allow, which likely serves to slow the rate of muscle atrophy (Geiser, 2004; Storey, 2015; Staples, 2016). However, there are additional mechanisms that are thought to slow or prevent muscle atrophy in these organisms. Increased production of antioxidants, such as superoxide dismutase, occurs in many hibernating and aestivating animals, and can prevent reactive oxygen species from disrupting protein synthesis or enabling proteolysis (Hudson et al., 2006; Allan and Storey, 2012; Powers et al., 2011; Vucetic et al., 2013). Activation of the exercise pathway gene *PGC-1α* in hibernating 13-lined ground squirrels shifts the composition of muscle fiber types towards a more fatigue-resistant

Journal of Experimental Biology

Journal of Experimental Biology (2017) 220, 2748-2756 doi:10.1242/jeb.154294

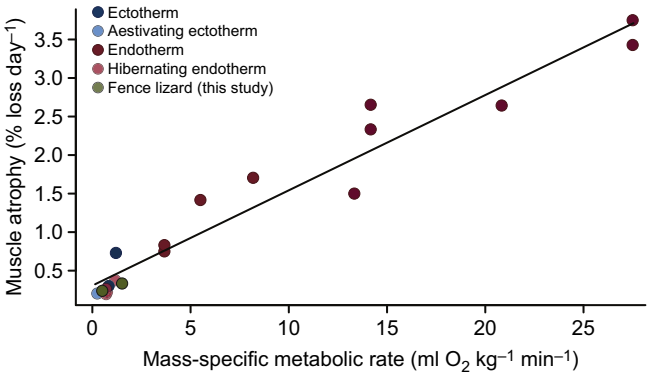

Fig. 6. Summary of data on muscle atrophy plotted against mass-specific metabolic rate. Different muscles atrophy at different rates even within the same animal, so only the muscle with the maximal rate of atrophy in each study was used to generate the plot. Disuse conditions include immobilization, aestivation, hibernation, hindlimb unweighting and denervation. Animals include ectotherms, endotherms and heterotherms. From left to right: aestivating burrowing frogs (Mantle et al., 2009), denervated fence lizards housed at 15°C (present study), hibernating black bear (Lohuis et al., 2007), hibernating and denervated black bear (Lin et al., 2012), hibernating ground squirrel (Wickler et al., 1991), immobilized turtle (McDonagh et al., 2004), hibernating hamster (Wickler et al., 1987), immobilized savannah monitor lizard (James Hicks and Amanda Szucsik, unpublished data), denervated fence lizards housed at 30°C (present study), immobilized humans (Veldhuizen et al., 1993), denervated black bear (Lin et al., 2012), immobilized dog (Bebout et al., 1993), denervated chicken (Jirmanová and Zelená, 1970), immobilized guinea pig (Maier et al., 1976), immobilized rat (Boyes and Johnston, 1979), hindlimb unweighted rat (Thomason and Booth, 1990), hindlimb unweighted hamster (Thomason and Booth, 1990), immobilized mouse (Soares et al., 1993) and hindlimb unweighted mouse (Thomason and Booth, 1990). There was a significant correlation between mass-specific metabolic rate and percentage atrophy (% daily atrophy=0.124×mass-specific metabolic rate+0.306, R^2=0.95, P<0.05).

profile, although it does not by itself prevent atrophy (Rourke et al., 2004; Bodine, 2013; Xu et al., 2013). Activation of the gene *SGK-1* in hibernating 13-lined ground squirrels inactivates *FoxO3a*, which normally mediates the atrophy response, and activates *mTOR*, which stimulates muscle growth (Andres-Mateos et al., 2013). The mechanisms found to resist muscle atrophy in hibernating animals extend well beyond those mentioned here and the full scope of these mechanisms was the focus of a recent review (Tessier and Storey, 2016). These mechanisms have received much attention recently, and have clear potential as therapeutic targets for slowing human muscle atrophy. The presence of these atrophy-resisting mechanisms does not slow the rate of atrophy in hibernators and aestivators beyond what would be predicted by metabolic rate alone but may serve to alter the pattern of atrophy.

Different muscles with similar fiber-type distributions and similar functions may still atrophy at different rates (Lieber, 2002). Though the molecular underpinnings of this are unclear, the relative activity level in the muscles before the application of a disuse stimulus may provide an explanation. Terrestrial mammals are generally more active than terrestrial ectothermic vertebrates (Bennett and Ruben, 1979). Therefore, mammalian leg muscles are acclimated to a much higher level of activity before they enter hibernation than the muscles of ectotherms. In the absence of the molecular mechanisms aimed at mitigating atrophy, mammalian muscle may incur significant atrophy even at a low metabolic rate as a result of the relatively large disuse stimulus. Additionally, antioxidant defenses and the activation of *PGC-1α* may serve to specifically preserve the slow oxidative tissues, which because of their high mitochondrial content produce reactive oxygen species at a higher rate than other muscle fiber types and are thus susceptible to faster rates of atrophy than other fiber types. Sparing of slow fibers would still result in normal patterns of atrophy in predominately fast muscles. Moreover, metabolic rate is suppressed globally, but that does not mean that all tissues are equally affected. In green-striped burrowing frogs, levels of citrate synthase, lactate dehydrogenase and cytochrome *c* oxidase were suppressed to different levels in different muscles during 6 and 9 months of aestivation (Mantle et al., 2010). Metabolic rate may therefore correlate with muscle atrophy on a muscle-specific level, and muscles that are the most important for locomotion may be preferentially spared. Finally, muscle atrophy may not result from disuse in hibernating mammals. In some cases, there seems to be a 'pre-programmed' shift in muscle properties that occurs during hibernation. Golden-mantled ground squirrels will hibernate at the same time of year regardless of environmental temperatures, yet the same pattern of atrophy in fast muscle fibers and sparing of slow muscle fibers is observed independent of temperature (Nowell et al., 2010). Seasonally induced muscle plasticity may be fundamentally different from disuse-induced atrophy and comparisons between these two mechanisms should be viewed with skepticism.

Conclusions

We found that in the ectothermic western fence lizard, *S. occidentalis*, muscle atrophy, after 6 weeks of denervation, is mitigated by a low metabolic rate to a similar degree to that seen in other vertebrates. We conclude that a reduced metabolic rate alone is sufficient to spare muscle protein over a long period of disuse. Though there are other mechanisms which may spare certain muscle fiber types or specific muscles, our findings indicate that any mechanism which can lower the metabolic rate of an animal can significantly slow muscle atrophy.

Acknowledgements

The authors are grateful to Erica Heinrich and Tim Bradley for guidance on measurements of metabolic rate. Sabine Moritz provided detailed techniques for histological staining. Gilbert Hernandez aided in animal and data collection. Natalie Holt provided valuable advice on isolated muscle experiments. James Hicks provided data for the monitor lizard data in Fig. 6. We also thank two anonymous reviewers, who provided feedback that greatly improved the manuscript.

Competing interests

The authors declare no competing or financial interests.

Author contributions

Conceptualization: J.B., E.A.; Methodology: J.B., E.A.; Validation: J.B., E.A.; Formal analysis: J.B.; Investigation: J.B.; Resources: J.B., E.A.; Writing - original draft: J.B.; Writing - review & editing: J.B., E.A.; Visualization: J.B., E.A.; Supervision: E.A.; Project administration: J.B., E.A.; Funding acquisition: J.B., E.A.

Funding

This work was supported by the National Science Foundation [grant number 1436476 to E.A.] and a Department of Education fellowship and a fellowship from the UC Irvine Francisco J. Ayala School of Biological Sciences to J.B.

References

Allan, M. E. and Storey, K. B. (2012). Expression of NF-κB and downstream antioxidant genes in skeletal muscle of hibernating ground squirrels, Spermophilus tridecemlineatus. *Cell Biochem. Funct.* **30**, 166-174.

Andres-Mateos, E., Brinkmeier, H., Burks, T. N., Mejias, R., Files, D. C., Steinberger, M., Soleimani, A., Marx, R., Simmers, J. L., Lin, B. et al. (2013). Activation of serum/glucocorticoid-induced kinase 1 (SGK1) is important to maintain skeletal muscle homeostasis and prevent atrophy. *EMBO Mol. Med.* **5**, 80-91.

Bakou, S., Cherel, Y., Gabinaud, B., Guigand, L. Wyers, M. (1996). Type-specific changes in fibre size and satellite cell activation following muscle denervation in two strains of turkey (Meleagris gallopavo). *J. Anat.* **188**, 677-691.

Bates, D., Mächler, M., Bolker, B. and Walker, S. (2015). Fitting linear mixed-effects models using lme4. *J. Stat. Softw.* **67**, 1-48.
Bebout, D. E., Hogan, M. C., Hempleman, S. C. and Wagner, P. D. (1993). Effects of training and immobilization on VO2 and DO2 in dog gastrocnemius muscle in situ. *J. Appl. Physiol.* **74**, 1697-1703.
Bennett, A. and Ruben, J. (1979). Endothermy and activity in vertebrates. *Science* **206**, 649-654.
Biewener, A. A. (2002). Future directions for the analysis of musculoskeletal design and locomotor performance. *J. Morphol.* **252**, 38-51.
Bodine, S. C. (2013). Hibernation: the search for treatments to prevent disuse-induced skeletal muscle atrophy. *Exp. Neurol.* **248**, 129-135.
Bonaldo, P. and Sandri, M. (2013). Cellular and molecular mechanisms of muscle atrophy. *Dis. Model. Mech.* **6**, 25-39.
Booth, F. W. (1982). Effect of limb immobilization on skeletal muscle. *J. Appl. Physiol.* **52**, 1113-1118.
Boyes, G. and Johnston, I. (1979). Muscle fibre composition of ratvastus intermedius following immobilisation at different muscle lengths. *Pflügers Arch.* **381**, 195-200.
Caiozzo, V. J. (2002). Plasticity of skeletal muscle phenotype: mechanical consequences. *Muscle Nerve* **26**, 740-768.
Caiozzo, V. J., Baker, M. J., Herrick, R. E., Tao, M. and Baldwin, K. M. (1994). Effect of spaceflight on skeletal-muscle - mechanical-properties and myosin isoform content of a slow muscle. *J. Appl. Physiol.* **76**, 1764-1773.
Caiozzo, V. J., Haddad, F., Baker, M. J., Herrick, R. E., Prietto, N. and Baldwin, K. M. (1996). Microgravity-induced transformations of myosin isoforms and contractile properties of skeletal muscle. *J. Appl. Physiol.* **81**, 123-132.
Dawson, W. R. and Bartholomew, G. A. (1956). Relation of oxygen consumption to body weight, temperature, and temperature acclimation in lizards Uta stansburiana and Sceloporus occidentalis. *Physiol. Zool.* **29**, 40-51.
Fitts, R. H., Metzger, J. M., Riley, D. A. and Unsworth, B. R. (1986). Models of disuse: a comparison of hindlimb suspension and immobilization. *J. Appl. Physiol.* **60**, 1946-1953.
Fox, J. and Weisberg, S. (2011). *An R Companion to Applied Regression*, 2nd edn. Thousand Oaks, CA: Sage.
Geiser, F. (2004). Metabolic rate and body temperature reduction during hibernation and daily torpor. *Annu. Rev. Physiol.* **66**, 239-274.
Hikida, R. S. and Bock, W. J. (1972). Effect of denervation on pigeon slow skeletal muscle. *Z. Zellforsch. mikrosk. Anat.* **128**, 1-18.
Hudson, N. J. and Franklin, C. E. (2002). Maintaining muscle mass during extended disuse: aestivating frogs as a model species. *J. Exp. Biol.* **205**, 2297-2303.
Hudson, N. J., Lehnert, S. A., Ingham, A. B., Symonds, B., Franklin, C. E. and Harper, G. S. (2006). Lessons from an estivating frog: sparing muscle protein despite starvation and disuse. *Am. J. Physiol. Regul. Integr. Comp. Physiol.* **290**, R836-R843.
James, R. S., Staples, J. F., Brown, J. C. L., Tessier, S. N. and Storey, K. B. (2013). The effects of hibernation on the contractile and biochemical properties of skeletal muscles in the thirteen-lined ground squirrel, Ictidomys tridecemlineatus. *J. Exp. Biol.* **216**, 2587-2594.
Jirmanová, I. and Zelená, J. (1970). Effect of denervation and tenotomy on slow and fast muscles of the chicken. *Z. Zellforsch. Mikrosk. Anat.* **106**, 333-347.
Lieber, R. L. (2002). *Skeletal Muscle Structure, Function & Plasticity: The Physiological Basis of Rehabilitation*. Philadelphia: Lippincott Williams & Wilkins.
Lin, D. C., Hershey, J. D., Mattoon, J. S. and Robbins, C. T. (2012). Skeletal muscles of hibernating brown bears are unusually resistant to effects of denervation. *J. Exp. Biol.* **215**, 2081-2087.
Lohuis, T. D., Harlow, H. J., Beck, T. D. I. and Iaizzo, P. A. (2007). Hibernating bears conserve muscle strength and maintain fatigue resistance. *Physiol. Biochem. Zool.* **80**, 257-269.
Maier, A., Crockett, J. L., Simpson, D. R., Saubert, C. W. and Edgerton, V. R. (1976). Properties of immobilized Guinea-pig hindlimb muscles. *Am. J. Physiol.* **231**, 1520-1526.
Mantle, B. L., Hudson, N. J., Harper, G. S., Cramp, R. L. and Franklin, C. E. (2009). Skeletal muscle atrophy occurs slowly and selectively during prolonged aestivation in Cyclorana alboguttata (Gunther 1867). *J. Exp. Biol.* **212**, 3664-3672.
Mantle, B. L., Guderley, H., Hudson, N. J. and Franklin, C. E. (2010). Enzyme activity in the aestivating Green-striped burrowing frog (Cyclorana alboguttata). *J. Comp. Physiol.* **180**, 1033-1043.
Marsh, R. L. and Bennett, A. F. (1986). Thermal dependence of contractile properties of skeletal muscle from the lizard Sceloporus occidentalis with comments on methods for fitting and comparing force-velocity curves. *J. Exp. Biol.* **126**, 63-77.
McDonagh, J. C., Callister, R. J., Favron, M. L. and Stuart, D. G. (2004). Resistance to disuse atrophy in a turtle hindlimb muscle. *J. Comp. Physiol.* **190**, 321-329.
Moritz, S. and Schilling, N. (2013). Fiber-type composition in the perivertebral musculature of lizards: Implications for the evolution of the diapsid trunk muscles. *J. Morphol.* **274**, 294-306.
Muleme, H. M., Walpole, A. C. and Staples, J. F. (2006). Mitochondrial metabolism in hibernation: metabolic suppression, temperature effects, and substrate preferences. *Physiol. Biochem. Zool.* **79**, 474-483.
Nowell, M. M., Choi, H. and Rourke, B. C. (2010). Muscle plasticity in hibernating ground squirrels (Spermophilus lateralis) is induced by seasonal, but not low-temperature, mechanisms. *J. Comp. Physiol.* **181**, 147-164.
Ohira, Y., Yoshinaga, T., Nomura, T., Kawano, F., Ishihara, A., Nonaka, I., Roy, R. R. and Edgerton, V. R. (2002). Gravitational unloading effects on muscle fiber size, phenotype and myonuclear number. *Life Gravity* **30**, 777-781.
Ohta, H., Okamoto, I., Hanaya, T., Arai, S., Ohta, T. and Fukuda, S. (2006). Enhanced antioxidant defense due to extracellular catalase activity in Syrian hamster during arousal from hibernation. *Comp. Biochem. Physiol. C Toxicol. Pharmacol.* **143**, 484-491.
Okamoto, I., Kayano, T., Hanaya, T., Arai, S., Ikeda, M. and Kurimoto, M. (2006). Up-regulation of an extracellular superoxide dismutase-like activity in hibernating hamsters subjected to oxidative stress in mid- to late arousal from torpor. *Comp. Biochem. Physiol. C Toxicol. Pharmacol.* **144**, 47-56.
Powers, S. K., Kavazis, A. N. and McClung, J. M. (2007). Oxidative stress and disuse muscle atrophy. *J. Appl. Physiol.* **102**, 2389-2397.
Powers, S. K., Smuder, A. J. and Criswell, D. S. (2011). Mechanistic links between oxidative stress and disuse muscle atrophy. *Antioxid Redox Signal.* **15**, 2519-2528.
Rourke, B. C. (2004). Cloning and sequencing of myosin heavy chain isoform cDNAs in golden-mantled ground squirrels: effects of hibernation on mRNA expression. *J. Appl. Physiol.* **97**, 1985-1991.
Rourke, B. C., Yokoyama, Y., Milsom, W. K. and Caiozzo, V. J. (2004). Myosin isoform expression and MAFbx mRNA levels in hibernating golden-mantled ground squirrels (Spermophilus lateralis). *Physiol. Biochem. Zool.* **77**, 582-593.
Schiaffino, S., Dyar, K. A., Ciciliot, S., Blaauw, B. and Sandri, M. (2013). Mechanisms regulating skeletal muscle growth and atrophy. *FEBS J.* **280**, 4294-4314.
Soares, J. M., Duarte, J. A., Carvalho, J. and Appell, H.-J. (1993). The possible role of intracellular Ca2+ accumulation for the development of immobilization atrophy. *Int. J. Sports Med.* **14**, 437-439.
Staples, J. F. (2014). Metabolic suppression in mammalian hibernation: the role of mitochondria. *J. Exp. Biol.* **217**, 2032-2036.
Staples, J. F. (2016). Metabolic flexibility: hibernation, torpor, and estivation. *Comp. Physiol.* **65**, 737-771.
Storey, K. B. (2015). Regulation of hypometabolism: insights into epigenetic controls. *J. Exp. Biol.* **218**, 150-159.
Tessier, S. N. and Storey, K. B. (2016). Lessons from mammalian hibernators: molecular insights into striated muscle plasticity and remodeling. *Biomol. Concepts* **7**, 69-92.
Thomason, D. B. and Booth, F. W. (1990). Atrophy of the soleus muscle by hindlimb unweighting. *J. Appl. Physiol.* **68**, 1-12.
Veldhuizen, J. W., Verstappen, F. T., Vroemen, J. P., Kuipers, H. and Greep, J. M. (1993). Functional and morphological adaptations following four weeks of knee immobilization. *Int. J. Sports Med.* **14**, 283-287.
Vucetic, M., Stancic, A., Otasevic, V., Jankovic, A., Korac, A., Markelic, M., Velickovic, K., Golic, I., Buzadzic, B., Storey, K. B. et al. (2013). The impact of cold acclimation and hibernation on antioxidant defenses in the ground squirrel (Spermophilus citellus): an update. *Free Radic. Biol. Med.* **65**, 916-924.
Wickler, S. J., Horwitz, B. A. and Kott, K. S. (1987). Muscle function in hibernating hamsters: a natural analog to bed rest? *J. Therm. Biol.* **12**, 163-166.
Wickler, S. J., Hoyt, D. F. and van Breukelen, F. (1991). Disuse atrophy in the hibernating golden-mantled ground squirrel, Spermophilus lateralis. *Am. J. Physiol.* **261**, R1214-R1217.
Winiarski, A. M., Roy, R. R., Alford, E. K., Chiang, P. C. and Edgerton, V. R. (1987). Mechanical properties of rat skeletal muscle after hind limb suspension. *Exp. Neurol.* **96**, 650-660.
Xu, R., Andres-Mateos, E., Mejias, R., MacDonald, E. M., Leinwand, L. A., Merriman, D. K., Fink, R. H. A. and Cohn, R. D. (2013). Hibernating squirrel muscle activates the endurance exercise pathway despite prolonged immobilization. *Exp. Neurol.* **247**, 392-401.
Young, K. M., Cramp, R. L. and Franklin, C. E. (2013). Each to their own: skeletal muscles of different function use different biochemical strategies during aestivation at high temperature. *J. Exp. Biol.* **216**, 1012-1024.